

US EPA ARCHIVE DOCUMENT

# Survey of Fractured Glacial Till Geotechnical Characteristics: Hydraulic Conductivity, Consolidation, and Shear Strength<sup>1</sup>

BARRY J. ALLRED, USDA-ARS Soil Drainage Research Unit, 590 Woody Hayes Drive, Columbus, OH 43210

**ABSTRACT.** A literature survey was conducted and fracture influences on engineering behavior of glacial till are summarized, specifically with regard to saturated hydraulic conductivity, consolidation potential, and shear strength. Saturated hydraulic conductivity is increased by fractures, in some cases by two or more orders of magnitude. This in turn results in larger values for the coefficient of consolidation,  $c_v$ , governing the rate of consolidation. A larger  $c_v$  corresponds to faster settlement. Modest increases in total settlement occur only if fractures are open. Fractures also have the overall effect of reducing shear strength. Upon removal of surface material by excavation or erosion, stress release and water infiltration lead to further decreases in shear strength. This strength loss process, called softening, is due mostly to a decrease in effective cohesion and usually takes years to complete. Once failure occurs, there is another substantial drop in shear strength to a residual value. This residual strength is a result of realignment of particles along the failure plane during shear, which decreases the effective angle of internal friction. The fracture impact magnitude on glacial till saturated hydraulic conductivity, consolidation potential, and shear strength is determined largely by aperture and spacing characteristics. As the number and/or size of fractures increase, changes in these geotechnical properties become more pronounced.

OHIO J SCI 100 (3/4):63-72, 2000

## INTRODUCTION

Greater than 30% of the Earth's land surface was covered by glaciers during the Pleistocene Epoch. Sediments deposited by glacial processes cover large areas of North America, Europe, and Asia. Till is the geologic term most frequently used in reference to these sedimentary deposits. Fractures of one form or another have been observed within tills from around the world. These fractures substantially influence the bulk hydraulic and mechanical behavior of this material. Within Ohio, fractured glacial tills are particularly common, and as a consequence, their geotechnical properties need to be carefully considered in design and before initiation of many construction projects, including landfills, open channels, building foundations, and roadway embankments to list a few.

## Classification of Glacial Till

Glacial till classification is generally based on mode of deposition. Basal till, also referred to as lodgement till, is deposited in the subglacial environment beneath the ice sheet. Two mechanisms have been proposed for release of sediment found in basal till: 1) a "plastering on" effect and 2) melting of debris-rich ice along the base of the glacier (Milligan 1976; Edil and Mickelson 1995; Benn and Evans 1998). Ablation tills are comprised of material accumulated in the supraglacial environment on the top of the ice and later deposited during melting associated with glacial retreat. Basal and ablation tills are both poorly sorted and commonly include grain sizes ranging from clay to gravel. Supraglacial environments typically contain an abundance of water capable of washing, transporting, and redepositing

sediment. This glacial material, called flow till, tends to be much better sorted than either basal or ablation tills (Benn and Evans 1998).

## Fracture Formation

Listed below are some of the natural mechanisms by which fractures (also known as joints, fissures, cracks, and so forth) are produced within glacial till (Boulton 1976; Kirkaldie and Talbot 1992):

- 1) vertical stress release caused by overburden reduction,
- 2) horizontal tensional stresses resulting from isostatic crustal rebound,
- 3) contraction from freezing,
- 4) shrinkage due to drying, and
- 5) induced failure from applied shear forces.

Sediment erosion along with removal or thinning of the glacial ice sheet are two ways to reduce overburden, thereby diminishing vertical stress and in turn producing horizontal fractures. Surficial, horizontally oriented tension stresses, resulting from isostatic crustal rebound, are most likely to generate vertical joints. Freezing and drying processes induce contraction, forming vertical fractures that exhibit a polygonal pattern in plan view. Till shrinkage due to drying can be caused by climate change and/or lowering of the water table. Horizontal ice flow generates substantial shear stress within the rock and sediment material beneath the glacier. If the ice flow induced shear stress exceeds rock/sediment shear strength, fractures are formed. The orientation of these fractures can be either vertical or sub-horizontal.

## OBJECTIVES AND PURPOSE

This paper was written with the goal of providing a compilation of previous research conducted on fractured glacial till geotechnical properties. To accomplish this

<sup>1</sup>Manuscript received 8 June 1999 and in revised form 20 December 1999 (#99-15).

task, an exhaustive literature search was conducted. Sources derived from books, journal articles, and conference proceedings came from a number of different disciplines including civil engineering, geology, and soil science.

## RESULTS AND DISCUSSION

Fractures can substantially influence the hydraulic and mechanical behavior of glacial till. Some of the characteristics most affected include hydraulic conductivity, consolidation potential, and shear strength. Construction projects within areas covered by glacial till often require careful consideration of fracture-induced changes in these soil characteristics. Perloff and Baron (1976) define soil in the engineering sense as all uncemented accumulations of solid particles produced by mechanical or chemical disintegration of rocks. The following three subsections provide a general discussion regarding fracture influence on glacial till hydraulic conductivity, consolidation potential, and shear strength.

### Saturated Hydraulic Conductivity

The saturated flow of water through a porous material, such as glacial till, is governed by Darcy's law:

$$q = -Ki \quad (1)$$

where  $q$  (L/T, Length/Time) is specific discharge,  $i$  (dimensionless) is the hydraulic gradient, and the hydraulic conductivity,  $K$  (L/T), is a proportionality constant between  $q$  and  $i$ . The value  $K$  is a function of both fluid and porous media attributes. Several mathematical models have been developed for  $K$  in fractured material. If flow is directed parallel to a set of smooth, continuous, planer fractures,  $K$  can be expressed:

$$K = K_{Matrix} + K_{Fractures} = \frac{kg}{\nu} + \frac{b^3g}{12\nu L} \quad (2)$$

where  $K_{Matrix}$  is the hydraulic conductivity of the porous media material between fractures,  $K_{Fractures}$  is the hydraulic conductivity of the fracture set,  $k$  (L<sup>2</sup>) is the intrinsic permeability of the porous media matrix,  $g$  (L/T<sup>2</sup>) is the gravitational acceleration constant,  $\nu$  (L<sup>2</sup>/T) is the kinematic viscosity,  $b$  (L) is the width of the fracture opening, also referred to as the fracture aperture, and  $L$  (L) is the mean distance between fractures. The equations used to model  $K$  increase in complexity as the fracture patterns themselves become more intricate. These more complex equations often address multiple fracture sets and therefore incorporate orientation along with aperture and spacing characteristics (de Marsily 1986).

Equation 2, and those similar to it, have limited practicality due to the difficulty in measuring  $b$ . However, it does serve to emphasize the strong positive correlation that exists between hydraulic conductivity and both aperture and number of fractures. For example, assume  $K_{Matrix} \ll K_{Fractures}$  which is commonly the case. Then by doubling the number of fractures,  $L$  is reduced by half, and  $K$  increases by a factor of two, assuming all other

variables remain constant. If  $b$  is doubled,  $K$  becomes larger by a factor of eight. This illustrates the strong effect that the fracture opening size has on hydraulic flow.

Fracture presence can significantly increase the overall saturated hydraulic conductivity of glacial tills (Hendry 1983; Garga 1988; Kirkaldie 1988; D'Astous and others 1989; Kirkaldie and Talbot 1992). Several studies indicate laboratory testing of small non-fissured samples can, in some cases, underestimate the overall hydraulic conductivity of fractured glacial till by two or more orders of magnitude (Grisak and others 1976; Hendry 1982; Keller and others 1986; McKay and others 1993). As an example, Keller and others (1986) reported that oedometer consolidation tests yielded an average hydraulic conductivity of  $3.5 \times 10^{-9}$  cm/s for small non-fissured glacial till samples obtained near Saskatoon, Saskatchewan. In comparison, the hydraulic conductivity of the bulk material containing fractures was measured using *in situ* slug tests and found to average  $5 \times 10^{-7}$  cm/s. McKay and others (1993) investigated fractured glacial till hydraulic conductivity near Sarnia, Ontario, and discovered *in situ* values from measuring infiltration into large trenches of  $1-3 \times 10^{-5}$  cm/s far exceeded the  $2 \times 10^{-8}$  cm/s average from laboratory oedometer consolidation tests on small non-jointed samples. Therefore, accurate field or laboratory estimation of saturated hydraulic conductivity requires the tested volume of undisturbed glacial till to be large enough to contain a representative distribution of fissures.

Obtaining valid hydraulic conductivity values can become a necessity in the proper evaluation of some geotechnical engineering problems. Due to rapid water movement through joints, some of the following problems are of particular concern in areas covered by fractured glacial tills:

- 1) increased slope instability due to rapid pore water pressure build-up along a potential failure plane,
- 2) seepage of water into a construction site excavation,
- 3) water loss from reservoirs and canals due to infiltration, and
- 4) rate of foundation settlement.

All of these problems can be magnified when stress release consequent to removal of surficial earth material is involved. Stress release causes fracture opening enlargement, thereby allowing increased water discharge through fissured glacial till material (Eq. 2). *In situ* hydraulic conductivity tests done before overburden removal may not account for the potential increase in flow rate. This brings up an important point that needs to be emphasized. The fracture aperture,  $b$ , is not constant but instead a function of local stress conditions. Therefore, the overall hydraulic conductivity,  $K$ , is likewise stress dependent.

Before the first problem can be addressed, the water source needs to be identified to determine whether it is from horizontal aquifer flow or vertical infiltration. One solution, regardless of the water source, involves utilization of horizontal drains to quickly dissipate any pore water pressure build-up along a potential failure plane.

Likewise, excessive pore pressures at the failure plane can sometimes be prevented from occurring in the first place by controlling vertical infiltration of surface water. Care must be taken when using capping material to reduce infiltration, because the extra weight can itself induce slope instability. Although expensive on a large scale, the second and third problems may be addressed using pressure grouting methods to seal fissures (Hausmann 1990). Discussion on the relationship between fractured glacial till hydraulic conductivity and the rate of foundation settlement is provided in the next section.

### Consolidation

Fractured glacial tills are typically characterized, at least to some extent, as being overconsolidated (Boulton 1976). The past stress history of a soil or sediment, such as glacial till, is important in determining future response to an applied load. A normally consolidated soil is one which has never experienced an effective stress greater than that it is experiencing at the present. On the other hand, an overconsolidated soil is one that has been subjected to greater effective stresses during the past than it is undergoing now. For an overconsolidated soil, the maximum effective stress ever applied is called the preconsolidation stress. The preconsolidation stress can be determined in the laboratory by plotting equilibrium measurements of soil sample void ratios,  $e$  (dimensionless), at different applied effective vertical stress values,  $\sigma'$  (M/LT<sup>2</sup>), (where M = mass), (Wray 1986). As shown in Figure 1, the preconsolidation pressure corresponds to a point taken on the  $e$  versus  $\sigma'$  curve where there is a transitional break in slope. The theoretical location of this point along the curve can be determined with a graphical procedure developed by Casagrande (1936).

The overconsolidation ratio, OCR, is used to gauge the amount of overconsolidation. The OCR is calculated as follows:

$$OCR = \frac{\sigma'_{pc}}{\sigma'_0} \quad (3)$$

where  $\sigma'_{pc}$  is the preconsolidation pressure, and  $\sigma'_0$  is the effective vertical stress due to current overburden. Theoretically, the OCR is always  $\geq 1$ . For normally consolidated soils, OCR = 1. Fractured glacial tills are usually overconsolidated and therefore have OCR values that are often substantially greater than 1.

A natural assumption, due to the presence of glacial overburden during deposition, is that basal tills are highly overconsolidated, and their preconsolidation pressure can be approximated by multiplying the specific weight of ice by the thickness of the ice sheet. Accordingly, the lack of overburden during formation suggests that ablation tills should exhibit normal consolidation, or at most, only a slight amount of overconsolidation. In reality however, the consolidation state of glacial till is much more complex. Actual basal till preconsolidation pressures are commonly much less than theoretical values calculated on the basis of assumed ice sheet thickness. Spatial variability of permeability and/or thermal conditions within sediments beneath the ice

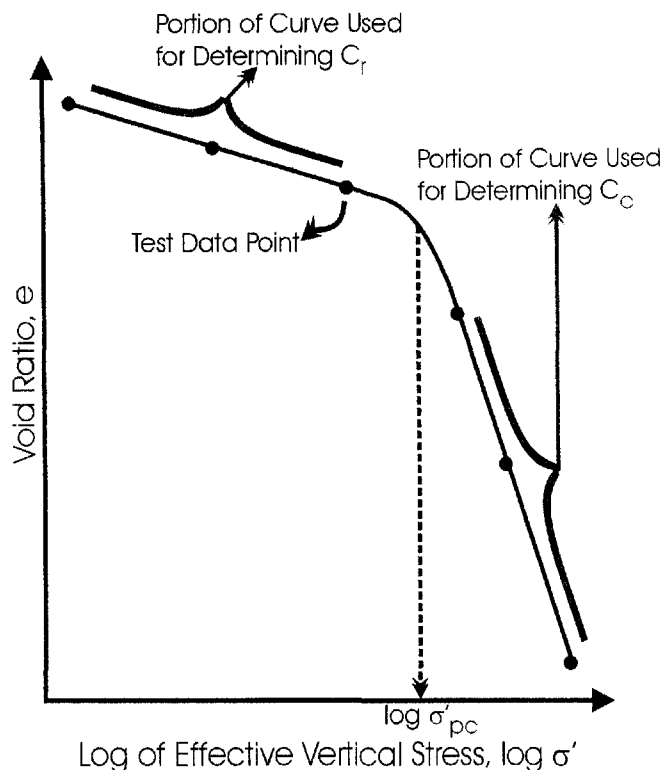


FIGURE 1. Plot of consolidation test data illustrating the relationship between the void ratio,  $e$ , and the common logarithm of effective vertical stress,  $\log \sigma'$ . Additionally, the overconsolidation pressure,  $\sigma'_{pc}$ , is shown along with portions of the curve from which the compression index,  $C_c$ , and recompression index,  $C_r$ , are determined.

sheet may prevent pore water pressure dissipation thereby limiting the total amount of consolidation which can occur (Boulton 1976; Edil and Mickelson 1995). OCR values for basal tills in southeastern Wisconsin were found to range between 2 and 31 (Edil and Mickelson 1995). With regard to ablation tills, high suction pressures generated during surface drying often resulted in this material being substantially overconsolidated. As an example of the effect due to drying, Mahar and O'Neill (1983) measured OCR values ranging from 1.5 to 10 for two desiccated clays in Texas. These Texas soils are non-glacial in origin, however their desiccation affected OCR values should be indicative of those for dried clayey till material. Consequently, knowledge regarding glacial till mode of deposition cannot always be used to provide clear indication as to consolidation state.

The OCR impacts the coefficient of earth pressure at rest,  $J_0$ , and in turn influences the orientation of hydraulically induced fractures.  $J_0$  is simply defined as the effective horizontal stress divided by the effective vertical stress. For normally consolidated soil (OCR = 1),  $J_0 < 1$ . Given the same soil material, the value of  $J_0$  will be greater for overconsolidated conditions (OCR > 1) than for normally consolidated conditions (Perloff and Baron 1976). For highly overconsolidated conditions (OCR >> 1), a value of  $J_0 > 1$  is often the case, meaning the effective horizontal stress is larger than the effective vertical stress.

Subsurface injection of high pressure slurries produce fractures in soil, thereby substantially increasing the overall hydraulic conductivity. This process is called hydraulic fracturing and can be used to enhance both pump-and-treat and *in situ* bioremediation efforts to remove contaminants from soil (Vesper and others 1994; Murdoch 1995). Some of the more innovative *in situ* cleanup technologies being tested involve placement of various constituents within hydraulic fractures. Field tests with zero valent iron ( $\text{Fe}^0$ ) and potassium permanganate ( $\text{KMnO}_4$ ) show promise with respect to removal of chlorinated organic compounds (Siegrist and others 1999). *In situ* experiments on low permeability soils provide evidence that pump-and-treat flow rates can be increased using electroosmosis in conjunction with emplacement of granular graphite within hydraulic fractures (Murdoch and Chen 1997).

The plane of a hydraulic fracture is positioned perpendicular to the direction of minimum confining stress. Within highly overconsolidated glacial material, the minimum confining stress direction is vertical ( $J_0 > 1$ ), and therefore the hydraulic fracture orientation is essentially horizontal (Murdoch 1995). Laboratory tests on a silty clay show that during formation, the induced cracks propagate outwards from the pressurized fluid source as a series of separated or overlapping lobes (Murdoch 1993a). These lobes eventually coalesce forming the main fracture plane. Locations on the main fracture plane where lobes have joined often exhibit ridge or step shaped features.

Constant injection rate laboratory tests by Murdoch (1993b) provide evidence of three stages in the development of a hydraulic fracture based on the relationship between injection fluid pressure and time. Before fracture initiation, fluid pressure increases at a linear rate. Once fracturing begins, injection fluid pressure keeps on increasing but at a continuously decreasing rate. This second stage reflects stable fracture propagation. When stable conditions exist, fracture propagation stops if fluid injection pressure ceases to increase. The third and final stage, where fluid injection pressure decreases with time, reflects unstable conditions. With unstable conditions, hydraulically induced fractures continue to propagate even if there is an injection pressure drop-off. Extensive laboratory and field testing of clayey silt and silty clay soil materials shows that hydraulic fracture propagation characteristics depend on several factors including moisture content, elastic modulus, tensile strength, hydraulic conductivity,  $J_0$ , and injection fluid density (Murdoch 1993a, 1993b, 1993c, 1995). Murdoch (1993c) developed a mathematical model describing hydraulic fracture propagation using principles of linear elastic fracture mechanics.

One of the most important considerations in geotechnical engineering is settlement of the soil material upon which a building structure rests. Both the amount and rate of settlement need to be taken into account. Excessive settlement amounts can result in broken utility lines along with appearance of cracks within a building structure. Fast settlement rates may not allow enough time for corrective measures to be undertaken. Primary

consolidation due to pore pressure dissipation is by far the largest component of settlement for a saturated cohesive soil, including many glacial tills located below the primary water table or within perched aquifers. The consolidation properties of greatest importance for quantifying settlement are the (re)compression index and the coefficient of consolidation. The compression index,  $C_c$  (dimensionless), and/or recompression index,  $C_r$  (dimensionless), govern the magnitude. The resulting consolidation of a saturated cohesive soil layer (Fig. 2), due to an increase in the applied stress,  $\sigma'_f - \sigma'_0$ , can be calculated using one of three equations (Perloff and Baron 1976; Wray 1986; Bowles 1988).

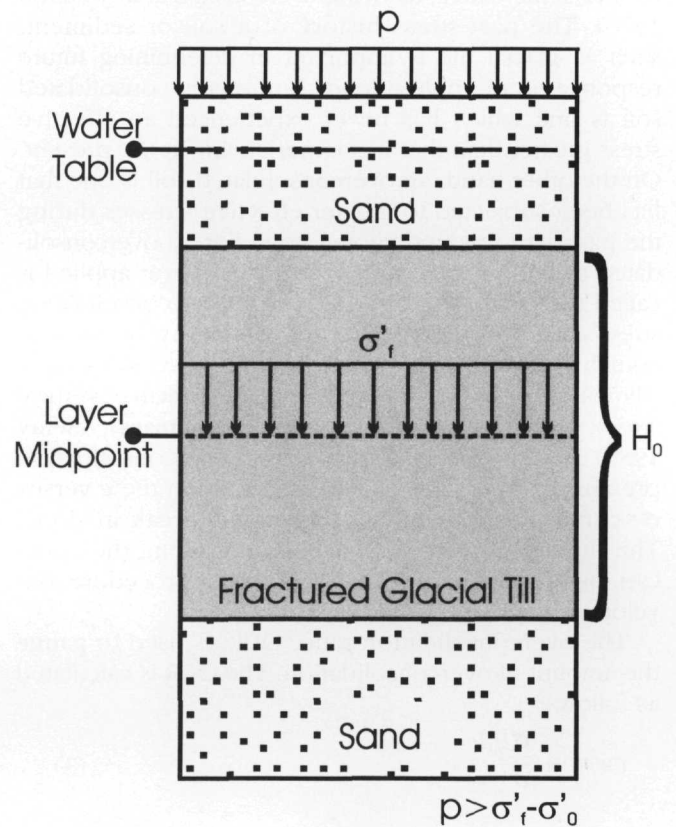


FIGURE 2. Schematic showing fractured glacial till layer prior to consolidation by a surface surcharge,  $p$ .

For a normally consolidated soil,

$$\Delta H = \frac{C_c H_0}{1 + e_0} \log \frac{\sigma'_f}{\sigma'_0} \quad (4)$$

For an overconsolidated soil with  $\sigma'_f$  less than  $\sigma'_{pc}$ ,

$$\Delta H = \frac{C_r H_0}{1 + e_0} \log \frac{\sigma'_f}{\sigma'_0} \quad (5)$$

For an overconsolidated soil with  $\sigma'_f$  greater  $\sigma'_{pc}$ ,

$$\Delta H = \frac{H_0}{1 + e_0} \left[ C_r \log \frac{\sigma'_0 + (\sigma'_{pc} - \sigma'_0)}{\sigma'_0} + C_c \log \frac{\sigma'_{pc} + (\sigma'_f - \sigma'_{pc})}{\sigma'_{pc}} \right] \quad (6)$$

$\Delta H$  (L) is the change in soil layer thickness due to consolidation,  $H_0$  is the initial soil layer thickness before surface load application,  $e_0$  is the original soil void ratio,

$\sigma'_f$  is the total vertical effective stress at the midpoint depth within the soil layer that results from an added surface surcharge,  $p$  (M/LT<sup>2</sup>) (Fig. 2). All other terms in Equations 4, 5, and 6 have been previously defined. Since overconsolidation conditions are typical, Equation 5 or 6 should be applied towards prediction of total thickness change in fractured glacial till. Highly overconsolidated (OCR >>1) tills tend to exhibit settlement amounts that are relatively small.

$C_c$  is substantially larger than  $C_r$ , and both are calculated using the following relationship:

$$C_c, C_r = \frac{-(e_2 - e_1)}{\left( \log \frac{\sigma'_2}{\sigma'_1} \right)}, \quad (7)$$

where  $-(e_2 - e_1)$  is the void ratio reduction caused by increasing effective vertical stress from  $\sigma'_1$  to  $\sigma'_2$ . All information needed to calculate  $C_c$  and  $C_r$  can be obtained from a plot  $e$  versus  $\log \sigma'$  (Fig. 1) derived from laboratory consolidation testing. For overconsolidated material,  $C_r$  is determined from the flat part of the curve corresponding to  $\sigma' < \sigma'_{pc}$ , while the steeper slope portion, having  $\sigma' > \sigma'_{pc}$ , is used for computing  $C_c$ . Because normally consolidated materials do not exhibit a slope break in  $e$  versus  $\log \sigma'$  curve, any two points,  $e_1, \sigma'_1$  and  $e_2, \sigma'_2$ , can be used to calculate  $C_c$  in this case.

The coefficient of consolidation,  $c_v$  (L<sup>2</sup>/T), determines the rate at which settlement will occur as governed by pore pressure dissipation. The settlement rate equation is (Perloff and Baron 1976; Wray 1986; Bowles 1988):

$$t_{\%} = \frac{T_{\%} H_D^2}{c_v}, \quad (8)$$

where  $t_{\%}$  (T) is the time required to achieve a certain percentage of settlement,  $T_{\%}$  (dimensionless) is the time factor associated with a specific settlement percent, and  $H_D$  (L) is the maximum drainage path distance. In turn, the coefficient of consolidation is expressed:

$$c_v = \frac{K}{m_v \gamma_w}, \quad (9)$$

where  $K$  is hydraulic conductivity,  $\gamma_w$  (M/LT<sup>2</sup>) is the specific weight of water, and  $m_v$  (LT<sup>2</sup>/M) is the coefficient of volume compressibility given by:

$$m_v = \frac{-(e_2 - e_1)}{(\sigma'_2 - \sigma'_1)(1 + e_1)}. \quad (10)$$

For jointed glacial till, Equation 2 shows  $K$  to be a function of fracture aperture and spacing. It follows from Equation 9  $c_v$  is likewise a function of fracture aperture and spacing. Therefore, larger aperture and/or decreased spacing between fractures should also correspond to faster settlement rates.

Fracture aperture and spacing impacts are further emphasized by the theoretical analysis presented in Table 1. Here, aperture and spacing characteristics are used to calculate  $K$  values. Estimates of  $c_v$  corresponding to  $K$  were then determined. Next, the time for 90% consolidation,  $t_{90\%}$ , was computed from the  $c_v$  estimates. Along with  $K$ ,  $c_v$ , and  $t_{90\%}$ , fracture porosity was also

calculated. In the scenario used for analysis, flow is parallel to two vertical sets of smooth, continuous, planar fractures intersecting at an angle of 90°. Aperture and spacing are considered the same for both sets. Apertures ranged from 0.0005 to 0.0025 to 0.0075 cm. With regard to fracture spacing, values of 5, 20, and 100 cm were analyzed. The chosen analysis conditions are similar to those of a clay-rich fractured glacial till deposit in Denmark described by Hinsby and others (1996). For this material, two sets of fractures were present and apertures calculated from ground water discharge rates and a modified version of Equation 2 ranged from 0.0035 to 0.0056 cm, while those determined from tracer tests ranged between 0.0013 and 0.012 cm. Fracture spacing for both sets was found to decrease from 20 cm near the surface to 5 cm at a depth of 50 cm. The analysis scenario also included a  $K_{Matrix}$  of  $1 \times 10^{-8}$  cm/s and a  $m_v$  of  $1 \times 10^{-8}$  (cm-s<sup>2</sup>)/gm. Both are reasonable values for glacial till (Garga 1988; McKay and others 1993). To calculate  $K$ , Equation 2 was modified to accommodate two sets of fractures through multiplication of the  $K_{Fractures}$  term by 2.

Table 1 suggests that fracture presence can significantly increase hydraulic conductivity. With no fractures,  $K$  equals  $1 \times 10^{-8}$  cm/s. Compared to this value, the fracture condition having the smallest aperture and widest spacing ( $b = 0.0005$  cm,  $L = 100$  cm) increases  $K$  by a factor of three.  $K$  is increased by five orders of magnitude for the largest aperture and closest spacing condition ( $b = 0.0075$  cm,  $L = 5$  cm). For the aperture and spacing values analyzed, fracture porosity is extremely low, ranging from  $1.0 \times 10^{-5}$  to  $3.0 \times 10^{-3}$ . This indicates, that for these aperture and spacing values, complete fracture closure by itself does not contribute substantially to the total amount of settlement. Fractures are, however, shown to be extremely important in determining the rate of settlement. With fractures absent, the  $c_v$  computed with Equation 9 is  $1 \times 10^{-3}$  cm<sup>2</sup>/s, and from Equation 8, the time for 90% consolidation is  $2.4 \times 10^3$  days ( $\approx 6.6$  years) given an  $H_D$  of 500 cm. The fracture condition with the smallest aperture and widest spacing gives a  $c_v$  of  $3.1 \times 10^{-3}$  cm<sup>2</sup>/s and a corresponding  $t_{90\%}$  of  $7.9 \times 10^2$  days ( $\approx 2.2$  years). The largest aperture and closest spacing fracture condition gives a  $c_v$  of  $1.4 \times 10^3$  cm<sup>2</sup>/s and a corresponding  $t_{90\%}$  of  $1.8 \times 10^{-2}$  days ( $\approx 26$  minutes).  $K$ ,  $c_v$ , and  $t_{90\%}$  estimates based on the largest aperture value of 0.0075 cm seem somewhat extreme and may be the result of simplifying model assumptions (such as smooth, continuous, planar, parallel fractures) which are not totally reflective of true natural conditions. Regardless, Table 1 still serves to emphasize the dramatic impact that fractures have on hydraulic conductivity, and in turn, the rate of consolidation.

Note from Equations 7 and 10 that the same variables are used to calculate  $m_v$  and both  $C_c$  and  $C_r$ . As  $m_v$  is reduced or enlarged, likewise  $C_c$  or  $C_r$ . In laboratory investigations with fissured London clay (Costa-Filho 1984; Garga 1988),  $m_v$  was observed to decrease as  $\sigma'$  increased. The study conducted by Garga (1988) also compared fissured and non-fissured samples,  $m_v^{(Fissured)}$  to be twice that of  $m_v^{(Non-fissured)}$  for  $\sigma'$  values below 400 kPa.

TABLE 1

*Fracture aperture and spacing impacts on soil properties.*

| Fracture Aperture, b (cm) | Fracture Spacing, L (cm) | Hydraulic Conductivity, $K^1$ (cm/s) | Fracture Porosity <sup>2</sup> | Coefficient of Consolidation, $c_v^3$ (cm <sup>2</sup> /s) | Time for 90% Consolidation, $t_{90\%}^4$ (days) |
|---------------------------|--------------------------|--------------------------------------|--------------------------------|--|---|
| 0 <sup>5</sup>            | $\infty^5$               | $1.0 \times 10^{-8}$                 | 0                              | $1.0 \times 10^{-3}$                                       | $2.4 \times 10^3$                               |
| .0005                     | 5                        | $4.2 \times 10^{-7}$                 | $2.0 \times 10^{-1}$           | $4.3 \times 10^{-4}$                                       | $5.7 \times 10^1$                               |
|                           | 20                       | $1.1 \times 10^{-7}$                 | $5.0 \times 10^{-5}$           | $1.1 \times 10^{-2}$                                       | $2.2 \times 10^2$                               |
|                           | 100                      | $3.0 \times 10^{-8}$                 | $1.0 \times 10^{-5}$           | $3.1 \times 10^{-3}$                                       | $7.9 \times 10^2$                               |
| .0025                     | 5                        | $5.1 \times 10^{-5}$                 | $1.0 \times 10^{-3}$           | $5.2 \times 10^0$  | $4.7 \times 10^{-1}$                            |
|                           | 20                       | $1.3 \times 10^{-5}$                 | $2.5 \times 10^{-1}$           | $1.3 \times 10^0$  | $1.9 \times 10^0$                               |
|                           | 100                      | $2.5 \times 10^{-6}$                 | $5.0 \times 10^{-5}$           | $2.6 \times 10^{-1}$                                       | $9.4 \times 10^0$                               |
| .0075                     | 5                        | $1.4 \times 10^{-3}$                 | $3.0 \times 10^{-3}$           | $1.4 \times 10^2$  | $1.8 \times 10^{-2}$                            |
|                           | 20                       | $3.4 \times 10^{-4}$                 | $7.5 \times 10^{-4}$           | $3.5 \times 10^1$  | $7.0 \times 10^{-2}$                            |
|                           | 100                      | $6.9 \times 10^{-5}$                 | $1.5 \times 10^{-1}$           | $7.0 \times 10^0$  | $3.5 \times 10^{-1}$                            |

<sup>1</sup>The hydraulic conductivity model assumes flow parallel to two sets of smooth, continuous, planer fractures intersecting at 90°. Aperture and spacing are the same for both sets.  $K_{Matrix} = 1 \times 10^{-8}$  cm/s,  $\nu = 1.007 \times 10^{-2}$  cm<sup>2</sup>/s at 20° C, and  $g = 981$  cm/s<sup>2</sup>.

<sup>2</sup>Fracture Porosity =  $b/L$ .

<sup>3</sup>Based on  $m_v = 1 \times 10^{-8}$  (cm<sup>2</sup>-s<sup>2</sup>)/gm and  $\gamma_w = 979$  gm/(cm<sup>2</sup>-s<sup>2</sup>) at 20° C.

<sup>4</sup>Based on  $T_{90\%} = 8.48 \times 10^{-1}$  and  $H_p = 500$  cm.

<sup>5</sup> $L = \infty$  and  $b = 0$  corresponds to the case in which no fractures are present.

However,  $\sigma'$  was increased beyond 400 kPa,  $m_{v(Fissured)}$  tended to coincide with  $m_{v(Non-fissured)}$ . The implications of these laboratory test results are important and listed as follows:

- 1) as depth beneath the surface increases, so too does *in situ* effective vertical stress, which results in closure of glacial till fractures,
- 2) when *in situ* effective vertical stress is relatively small, the values of the consolidation parameters,  $m_v$ ,  $C_c$ , and  $C_r$ , are higher for a glacial till with open fissures than the same glacial till without fissures,
- 3) when *in situ* effective vertical stress is relatively large, the values of the consolidation parameters,  $m_v$ ,  $C_c$ , and  $C_r$ , are comparable between a glacial till with *closed* fissures and the same glacial till without fissures,
- 4) if open fissures are present, total settlement increases with increased  $C_c$  or  $C_r$ , and
- 5) if fissures are closed, they have no affect on total settlement.

The term "closed" simply refers to a substantial reduction in aperture, but it does not imply that the fracture has been sealed off as a preferential flow path for water.

It has been observed that actual field settlement rates for fissured clays are substantially greater than those predicted by laboratory testing (Garga 1988). Knowledge of commonly used laboratory procedures provides a clue as to the difference between predicted and observed values. The consolidation parameters,  $c_v$ ,  $m_v$ ,  $C_c$ , and  $C_r$ , are typically determined with oedometer tests on small, 6.4-7.6 cm diameter, 2.5 cm thick, non-

fissured samples. If obtained from a fractured glacial till, these samples will have a hydraulic conductivity,  $K$ , much lower than representative of the bulk material. The consequence is that  $c_v$  is also underestimated, since it is a function of  $K$  (Eq. 9). Consequently, the overall result is that the consolidation time is overestimated (Eq. 8). For glacial till with closed fractures ( $m_{v(Fissured)} = m_{v(Non-fissured)}$ ), Garga (1988) recommends the following relationship for accurately estimating the coefficient of consolidation:

$$C_{v(Field)} = \frac{K_{Field}}{m_{v(Laboratory)} \gamma_w} \quad (11)$$

where  $K_{Field}$  is hydraulic conductivity measured in the field using well tests capable of sampling a representative volume of material.

Settlement is a major concern in a wide range of construction projects. With regard to fractured glacial till under saturated conditions, the following conclusions can be drawn from discussion in the previous three paragraphs:

- 1) at depth, where fractures are likely to be closed, oedometer tests on small non-fissured samples will provide accurate estimates of  $C_c$  or  $C_r$  needed to compute total settlement,
- 2) nearer the surface, where fractures tend to be open,  $C_c$  or  $C_r$  should be estimated using alternative methods such as laboratory pore pressure dissipation experiments on large samples (Garga 1988), or even better, *in situ* field testing using either a piezometric cone penetrometer or a self boring pressuremeter (Bowles 1988),



- 3) the consolidation rate in material having closed fractures can be resolved using Equation 11 to calculate  $c_v$ ,
- 4) referring to Equation 9,  $c_v$  is increased with open fractures because the orders of magnitude jump in  $K$  far outweighs the modest gains for  $m_v$ , and
- 5) where fractures are open,  $c_v$  is best determined *in situ* with either a piezometric cone penetrometer or a self boring pressuremeter (Bowles 1988).

Statistical analysis of values obtained from several spatially distributed piezometric cone penetrometer or self boring pressuremeter tests may be required in order to get representative estimates of  $c_v$ ,  $m_v$ ,  $C_c$ , and  $C_r$ .

When total settlement amounts are expected to be excessive, one of the remedies commonly employed is preloading. Preloading preempts settlement through placement of a temporary surcharge on the ground prior to building a planned structure (Hausmann 1990). Here, fractures in glacial tills are an advantage, since they reduce the time required for preloading. However, if excessive settlement is not initially accounted for, fractures can become a disadvantage, since they reduce the time available for taking corrective action.

### Shear Strength

Soil shear strength is the primary consideration in the analysis of many geotechnical engineering problems, particularly those involving slope stability and foundation bearing capacity. The stability of both natural and constructed slopes is governed by soil shear strength. When an applied shear force exceeds the resisting force contributed by integrating the shear strength over the potential slip surface, the slope fails resulting in either a slump or a landslide with the potential for loss of property or even life. Bearing capacity is defined as the maximum vertical pressure that can be applied to a soil surface by a shallow foundation component, such as a spread footing. Once bearing capacity is exceeded, shear failure of the soil beneath the foundation will occur causing substantial damage to the overlying structure.

The relationship for soil shear strength,  $s$  (M/LT<sup>2</sup>), based on total stress is:

$$s = c + \sigma_n \tan \phi \quad (12)$$

or in terms of effective stress:

$$s = c' + \sigma'_n \tan \phi' = c' + (\sigma_n - \mu) \tan \phi' \quad (13)$$

where  $\sigma_n$  is the total normal stress on the failure plane along which shear occurs, the effective normal stress,  $\sigma'_n$ , equals the total normal stress minus pore water pressure ( $\sigma_n - \mu$ ),  $c$  and  $c'$  (M/LT<sup>2</sup>) are the respective total or effective values of soil cohesion, and  $\phi$  and  $\phi'$  (dimensionless) are the respective total and effective values of the internal friction angle.

Cohesion and internal friction angle are soil properties, and both can be measured in the laboratory using direct shear or triaxial compression tests. In these tests, displacement along a failure plane is monitored with respect to applied shear stress. The laboratory soil

samples used to investigate shear strength are ordinarily quite small (less than 1000 cm<sup>3</sup>) and commonly chosen not to contain fissures. Figure 3 typifies results obtained from either direct shear or triaxial compression tests along with illustrating the shear strength difference between the normally consolidated and overconsolidated states of the same soil. Given similar experimental conditions, such as deformation rate and applied normal stress, the peak strength for an overconsolidated soil is greater than that of the same soil normally consolidated. Peak shear strength occurs just before failure. Afterwards, shear strength trends towards a residual value once particle realignment along the failure plane is complete. The residual strength of a soil is constant regardless of whether it is normally consolidated or overconsolidated. For a particular consolidation state, peak strength or in some cases the residual strength from several tests are then plotted against total or effective normal stress in order to graphically determine cohesion and angle of internal friction (Fig. 4).

The remaining discussion focuses solely on saturated cohesive soils, which includes glacial tills located beneath the primary water table or within perched aquifers. The measured values of cohesion and internal friction angle are both strongly influenced by test conditions. Generally, one of three sets of test conditions is used to study soil behavior during shear.

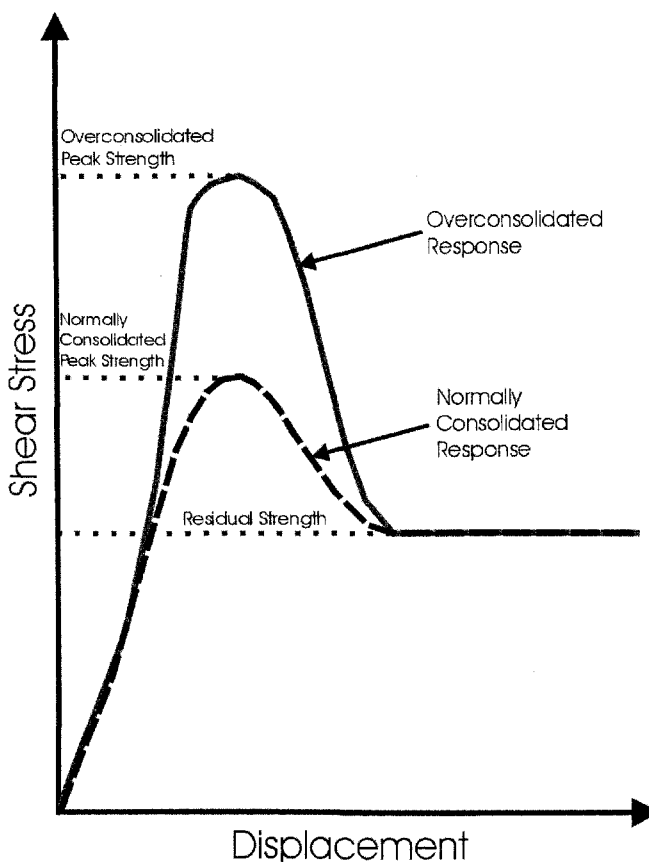


FIGURE 3. Illustration of typical results from a direct shear or triaxial compression test conducted on a soil sample under constant normal stress. The response of both the normally and overconsolidated states are shown.



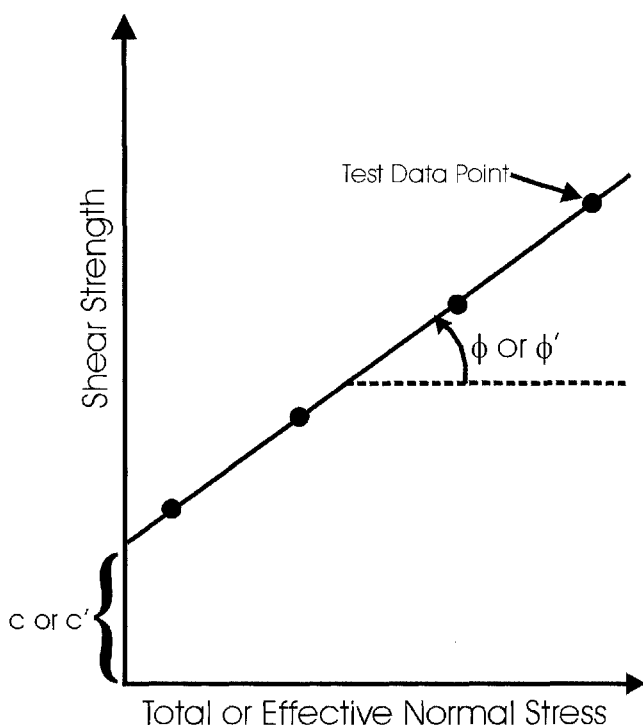


FIGURE 1. The cohesion and internal friction angle components of the shear strength equation are obtained from regression analysis of the results from several shear tests. Peak strength values are usually plotted, although graphs based on residual strengths are also common.

**Unconfined, Undrained (UU):** In tests conducted under these conditions, there is no confining pressure on the sample, and the fast rate of load application prevents pore pressure dissipation. UU tests represent the short term response to stress change, and the results ideally give  $c > 0$  and  $\phi = 0$ .

**Confined, Undrained (CU):** The sample is allowed to reach equilibrium with confining pressure before rapid application of shear force to produce failure. Pore pressure dissipation is thus prevented, and results give  $c > 0$  and  $\phi > 0$ .

**Confined, Drained (CD):** The sample is in equilibrium with confining pressure prior to the application of load at a rate slow enough to allow pore water pressure dissipation. CD tests represent the long term response to stress change. Test results for normally consolidated soil give  $c' \approx 0$  and  $\phi' > 0$ . For overconsolidated soil,  $c' > 0$  and  $\phi' > 0$ .

It has long been observed that the shear strength of dense, fractured glacial till is often much less than what would be expected for an overconsolidated material. An extreme example is the valley of the Saskatchewan River south of Saskatoon, Canada, where slides in dense, fractured glacial till occur repeatedly on relatively flat slopes having an average vertical to horizontal ratio of only 1:15 (Terzaghi and Peck 1967). Consequently, fracture impacts need to be addressed for accurate geotechnical evaluation of glacial till shear strength.

The measured shear strength of a fractured soil material depends on the size of the test specimen. Bishop and Little (1967) showed that fissured London clay shear

strength determined from an undrained *in situ* shear box test on a 61 cm by 61 cm square sample was only 55% of that given by a laboratory UU triaxial test on a 4 cm diameter non-fractured specimen. The shear strength of a sample taken from fractured soil material always falls within well defined upper and lower limits (Lo 1970). Maximum shear strength is obtained with test specimens containing no fissures. This is often referred to as the intact shear strength. Samples having a fissure oriented along the failure plane exhibit minimum shear strength. This is called the fissure strength and it has a value only slightly above the residual strength. Lo (1970) developed the following relationship for UU shear strength based on sample size:

$$s = s_m + (s_0 - s_m)e^{-\alpha(A-A_0)^\beta} \quad \text{for } A > A_0 \quad (14)$$

where  $A$  is the failure plane area for the test specimen,  $s$  the UU shear strength of the sample having a failure plane area  $A$ ,  $s_0$  is the intact UU shear strength,  $s_m$  is the effective UU shear strength of the overall fractured soil mass ( $A \rightarrow \infty$ ), and  $A_0$  is the area of the failure plane at and below which value the intact UU strength is measured. The quantities  $\alpha$  and  $\beta$  are parameters which increase in value with size and number of fractures. As  $\alpha$  and  $\beta$  get larger, the sample size at which  $s$  approaches  $s_m$  becomes smaller. Lo (1970) states that the value  $s_m$  is less than the intact shear strength but, except for special circumstances, substantially greater than the fissure strength. Results from laboratory UU tests on several samples of different size can be used with Equation 14 to estimate the overall effective UU shear strength,  $s_m$ . This is the quantity most often needed in evaluating shear strength under rapid loading conditions, examples of which include a silo quickly filled with grain or water added to a large above ground storage tank over a short period of time.

Fractures also present problems with respect to long term shear strength. In materials such as overconsolidated fractured glacial till, shear strength decreases over time following excavation or erosion of overburden (Terzaghi and Peck 1967; Duncan and Dunlop 1969). This strength reduction process, called softening, has been described by Terzaghi and Peck (1967) as follows:

- 1) stress release due to overburden reduction opens pre-existing fissures,
- 2) this facilitates water entry which softens material adjacent to fissures,
- 3) the softening process itself is caused by unequal swelling with the overall effect being production of new fissures, and
- 4) the resulting breakdown in structure leaves a soil mass that has been transformed into a soft matrix containing hard cores.

Fracture aperture and spacing undoubtedly influence the rate of softening, however to what degree is uncertain. Complete softening usually takes years to develop, but in rare cases can occur quickly in a matter of days. Both Terzaghi and Peck (1967) and Duncan and Dunlop (1969) document cases of engineered slopes which failed 20 to 80 years after construction. At the other

extreme, laboratory tests conducted by Stark and Duncan (1991) showed that a desiccation-fractured overconsolidated clay from the San Luis Dam site in California quickly reached a fully softened state within hours or days after being soaked with water. Although more research is needed, these test results may indicate quick softening upon rewetting for materials, such as many ablation tills, that have been overconsolidated and fractured by desiccation.

On approaching the fully softened state, the strength of the fractured soil mass trends towards that of the normally consolidated peak value (Skempton 1970). However, there are cases, as indicated by tests on highly plastic material with liquid limit values between 40% and 130% (Stark and Eid 1997), where total shear failure did not occur until soil strength had been reduced to a value halfway between peak normally consolidated and residual values. Obviously, undisturbed normally consolidated samples cannot be obtained from an overconsolidated fractured glacial till. However, the peak value from a CD test on a remolded normally consolidated sample can be used instead to represent the fully softened shear strength (Skempton 1970; Stark and Eid 1997). Once a slump or landslide has occurred, shear strength along the failure plane equals the residual value (Skempton 1970).

In summation, the process of softening typically results in fractured glacial till shear strength gradually decreasing over time until eventually leveling off at a point near the normally consolidated peak value. Shear force may exceed the resisting force at any time during the softening process. When this happens, failure occurs and the fractured glacial till shear strength becomes equal to that of the residual value. Figure 5 provides a graphical illustration of the changes that take place in the effective components of shear strength,  $c'$  and  $\phi'$ , as fractured glacial till softens and then fails. During softening,  $\phi'$  remains somewhat constant and  $c'$  trends towards zero, while after failure, loss in shear strength is due mostly to reduction in  $\phi'$  (Skempton 1970). Particle size distribution and Atterberg limits both influence the decrease that occurs in shear strength components. Stark and Eid (1997) determined that the difference in  $\phi'$  between the fully softened and residual strength states is minor for low plasticity soils having liquid limits below 30%. Fracture infilling by fine grained particulate material or chemical precipitation may influence the softening process or alter the residual strength, but to what extent is unclear at this time.

There are three different time frames to consider regarding engineering design decisions based on fractured glacial till shear strength.

**Short Term** (days or weeks): Equation 14 can be used to determine UU shear strength for quick loading conditions near the surface. Results from several UU tests on different size specimens are needed in order to determine  $\alpha$ ,  $\beta$  and  $s_m$ . In most cases, the potential failure plane is large enough that  $s_m$  can be employed in design considerations. However, if the failure plane is small, as may be the case beneath some foundation footings, the  $s$  value calculated from Equation 14 should

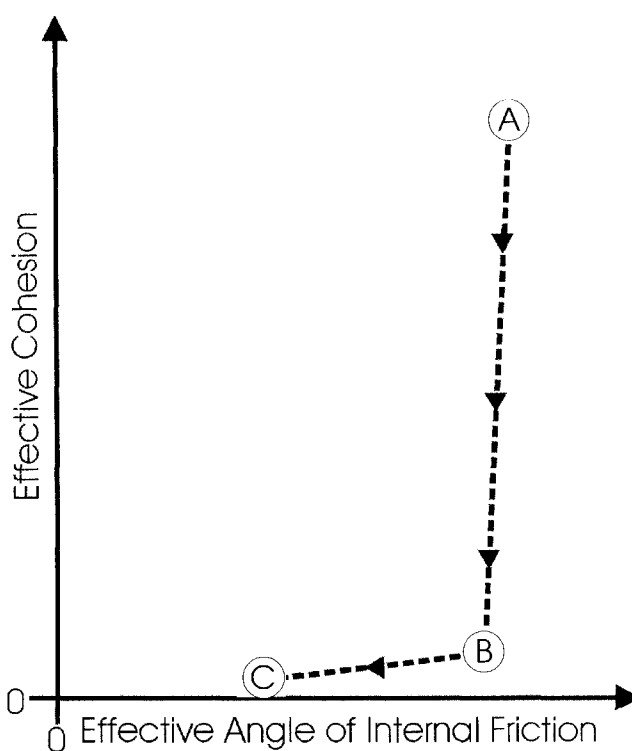


FIGURE 5. Fractured glacial till shear strength reduction over time plotted with respect to changes in effective cohesion and internal friction angle components. Point A is the initial state, B is the fully softened state, and C represents the conditions present after shear failure has occurred

be used instead.

**Long Term – Prior to Initial Failure (Years):** The design strength representing the fully softened state applies and is usually estimated by the peak value from a CD test conducted on a remolded normally consolidated sample. For highly plastic material with liquid limits ranging between 40% and 130%, a more conservative approach is to use the average of the remolded normally consolidated peak and residual strengths.

**Long Term – After Initial Failure (Years):** In areas where there have been previous slope failures, the residual shear strength is used for design purposes. This value can be determined from CD tests on any sample taken from the soil mass, undisturbed or remolded and normally consolidated or overconsolidated.

If the natural shear strength of the fractured glacial till material is not sufficient, protective measures need to be adopted. Rapid infiltration of water through cracks can cause pore pressure build-up resulting in decreased shear strength (Eq. 13) along a potential failure plane. As previously stated in the hydraulic conductivity section, there are two ways of inhibiting pore pressure build-up, horizontal drains to remove existing water and impervious capping material placed at the surface to limit vertical infiltration. By using impervious capping material to reduce the amount of water entering the subsurface, softening of overconsolidated fractured glacial till is also delayed, thereby allowing high shear strength levels to be maintained over a longer period of time. In some cases, increasing the natural shear strength is required.

This can be accomplished in one of two ways. One method involves filling cracks with cement using pressure grouting methods (Hausmann 1990). As an alternative, vegetation having roots extending below the failure plane can be established for the purpose of anchoring a slide mass to a hillslope (Sidle and others 1985).

### SUMMARY

Fractured glacial tills are common throughout the midwestern United States. Fracture characteristics such as size of openings and the spacing between them both influence overall engineering behavior. Consequently, correct geotechnical design decisions in places such as Ohio often require careful consideration of fracture impacts on hydraulic and mechanical properties of glacial till. Most important are the saturated hydraulic conductivity, consolidation potential, and shear strength effects.

**Saturated Hydraulic Conductivity:** Fractures increase the overall hydraulic conductivity of glacial till, in some cases by two or more orders of magnitude.

**Consolidation:** Settlement occurs at a faster rate when fractures are present. If fractures are open, a modest increase in total settlement is possible.

**Shear Strength:** Glacial till fractures decrease overall shear strength. After excavation or erosion of surface material, stress release and water infiltration lead to further reductions in overall shear strength. This process is called softening and can take years to complete. Once failure occurs, there is another substantial drop in shear strength to the residual value.

Because fractured glacial tills are so widespread throughout the northern hemisphere, more investigation of their properties is warranted, particularly with regard to long term shear strength conditions in natural and constructed slopes. Only through increased understanding can the engineering problems associated with fractured glacial tills be adequately addressed.

### LITERATURE CITED

- Benn DI, Evans DJA. 1998. *Glaciers and glaciation*. London: Arnold Publ. 734 p.
- Bishop AW, Little AL. 1967. The influence of size and orientation of the sample on the apparent strength of the London Clay at Maldon, Essex. *Proceedings of the Geotechnical Conference on Shear Strength of Natural Soils and Rocks*. Oslo, Norway, 19-22 Sept 1967. Oslo: Norwegian Geotechnical Institute. Vol 1. p 89-96.
- Boulton GS. 1976. The development of geotechnical properties in glacial tills. In: RF Legget, editor, *Glacial Till*. Ottawa: The Royal Society of Canada. Special Publication No. 12. p 292-303.
- Bowles JE. 1988. *Foundation analysis and design*, 4th ed. New York: McGraw-Hill. 1004 p.
- Casagrande A. 1936. The determination of the pre-consolidation load and its practical significance. 1st International Conference on Soil Mechanics and Foundation Engineering, 22-26 June 1936, Cambridge, MA. Cambridge (MA): Harvard University. Vol 3. p 60-4.
- Costa-Filho LM. 1984. A note on the influence of fissures on the deformation characteristics of London clay. *Geotechnique* 34:268-72.
- D'Astous AY, Ruland WW, Bruce JRG, Cherry JA, Gillham RW. 1989. Fracture effects in the shallow groundwater zone in weathered Samia-area clay. *Can Geotech J* 26:43-56.
- de Marsily G. 1986. *Quantitative hydrogeology: groundwater hydrology for engineers*. San Diego (CA): Academic Pr. 440 p.
- Duncan JM, Dunlop P. 1969. Slopes in stiff-fissured clays and shales. *J Soil Mechanics and Foundations Div ASCE* 95(2):467-92.
- Edil TB, Mickelson DM. 1995. Overconsolidated glacial tills in eastern Wisconsin. *Transport Resrch Rec* 1479:99-106.
- Garga VK. 1988. Effect of sample size on consolidation of a fissured clay. *Can Geotech J* 34:76-84.
- Grisak GE, Cherry JA, Vonhof JA, Blumele JP. 1976. Hydrogeologic and hydrochemical properties of fractured till in the interior plains region. In: RF Legget, editor, *Glacial till*. Ottawa: The Royal Society of Canada. Special Publication No. 12. 269-91.
- Hausmann MR. 1990. *Engineering principles of ground modification*. New York: McGraw-Hill. 632 p.
- Hendry MJ. 1982. Hydraulic conductivity of a glacial till in Alberta. *Ground Water* 20(2):162-9.
- Hendry MJ. 1983. Groundwater recharge through a heavy-textured soil. *J Hydrology* 63:201-9.
- Hinsby K, McKay LD, Jorgensen P, Lenczewski M, Gerba CP. 1996. Fracture aperture measurements and migration of solutes, viruses, and immiscible creosote in a column of clay-rich till. *Ground Water* 34(6):1065-75.
- Keller CK, Van der Kamp G, Cherry JA. 1986. Fracture permeability and groundwater flow in a clayey till near Saskatoon, Saskatchewan. *Can Geotech J* 23:229-40.
- Kirkaldie L. 1988. Potential contaminant movement through soil joints. *Bull Assoc Engineer Geol* 25(4):520-4.
- Kirkaldie L, Talbot JR. 1992. The effects of soil joints on soil mass properties. *Bull Assoc Engineer Geol* 29(4):415-20.
- Lo KY. 1970. The operational strength of fissured clays. *Geotechnique* 20(1):57-74.
- Mahar IJ, O'Neill MW. 1983. Geotechnical characterization of desiccated clay. *J Geotech Eng ASCE* 109(1):56-71.
- McKay LD, Cherry JA, Gillham RW. 1993. Field experiments in a fractured clay till hydraulic conductivity and fracture aperture. *Water Resources Research* 29(4):1149-62.
- Milligan V. 1976. Geotechnical aspects of glacial tills. In: RF Legget, editor, *Glacial till*. Ottawa: The Royal Society of Canada. Special Publication No. 12. 269-91.
- Murdoch LC. 1993a. Hydraulic fracturing of soil during laboratory experiments. Part 1, Methods and observations. *Geotechnique* 43(2):255-65.
- Murdoch LC. 1993b. Hydraulic fracturing of soil during laboratory experiments. Part 2, Propagation. *Geotechnique* 43(2):267-76.
- Murdoch LC. 1993c. Hydraulic fracturing of soil during laboratory experiments. Part 3, Theoretical analysis. *Geotechnique* 43(2):277-87.
- Murdoch LC. 1995. Forms of hydraulic fractures created during a field test in overconsolidated glacial drift. *Qtrly J Engineer Geol* 28:23-35.
- Murdoch LC, Chen J. 1997. Effects of conductive fractures during *in-situ* electroosmosis. *J Hazard Materials* 55:239-62.
- Perloff WH, Baron W. 1976. *Soil mechanics: principles and applications*. New York: J Wiley. 745 p.
- Sidle RC, Pearce AJ, O'Loughlin CL. 1985. *Hillslope stability and land use*. Water Resources Monograph 11. Washington (DC): American Geophysical Union. 140 p.
- Siegrist RL, Lowe KS, Murdoch LC, Case TL, Pickering DA. 1999. *In situ* oxidation by fracture emplaced reactive solids. *J Environ Engineer* 125(5):429-40.
- Skempton AW. 1970. First-time slides in over-consolidated clays. *Geotechnique* 20(4):320-4.
- Stark TD, Duncan JM. 1991. Mechanisms of strength loss in stiff clays. *J Geotech Eng ASCE* 117(1):139-54.
- Stark TD, Eid HT. 1997. Slope stability in stiff fissured clays. *J Geotech Geoenviron Eng* 123(4):335-43.
- Terzaghi K, Peck RB. 1967. *Soil mechanics in engineering practice*. New York: J Wiley. 729 p.
- Vesper SJ, Narayanaswamy M, Murdoch LC, Davis-Hoover WJ. 1994. Hydraulic fracturing to enhance *in situ* bioreclamation of subsurface soils. In: LC Murdoch, M Narayanaswamy, M Sayles, editors, *Applied biotechnology for site remediation*. Boca Raton (FL): Lewis Publ. p 36-48.
- Wray WK. 1986. *Measuring engineering properties of soil*. Englewood Cliffs (NJ): Prentice-Hall. 276 p.